324

Biological characterization of AT7519, a small-molecule inhibitor of cyclin-dependent kinases, in human tumor cell lines

Matthew S. Squires, Ruth E. Feltell,
Nicola G. Wallis, E. Jonathan Lewis,
Donna-Michelle Smith, David M. Cross,
John F. Lyons, and Neil T. Thompson

Astex Therapeutics Ltd., Cambridge, United Kingdom

Abstract

Cyclin-dependent kinases (CDK), and their regulatory cyclin partners, play a central role in eukaryotic cell growth, division, and death. This key role in cell cycle progression, as well as their deregulation in several human cancers, makes them attractive therapeutic targets in oncology. A series of CDK inhibitors was developed using Astex's fragment-based medicinal chemistry approach, linked to high-throughput X-ray crystallography. A compound from this series, designated AT7519, is currently in early-phase clinical development. We describe here the biological characterization of AT7519, a potent inhibitor of several CDK family members. AT7519 showed potent antiproliferative activity (40-940 nmol/L) in a panel of human tumor cell lines, and the mechanism of action was shown here to be consistent with the inhibition of CDK1 and CDK2 in solid tumor cell lines. AT7519 caused cell cycle arrest followed by apoptosis in human tumor cells and inhibited tumor growth in human tumor xenograft models. Tumor regression was observed following twice daily dosing of AT7519 in the HCT116 and HT29 colon cancer xenograft models. We show that these biological effects are linked to inhibition of CDKs *in vivo* and that AT7519 induces tumor cell apoptosis in these xenograft models. AT7519 has an attractive biological profile for development as a clinical candidate, and the tolerability and efficacy in animal models compare favorably with other CDK inhibitors in clinical development. Studies described here formed the biological rationale for investigating the potential therapeutic benefit of AT7519 in cancer patients. [Mol Cancer Ther 2009;8(2):324–32]

Introduction

Progression through the various phases of the eukaryotic cell cycle has been shown to be critically dependent on a family of proteins known as cyclin-dependent kinases (CDK) and their cognate regulatory partners termed cyclins (reviewed in refs. 1, 2). Formation of specific CDK/cyclin complexes controls passage through discrete cell cycle checkpoints and failure of this process can lead to cell cycle arrest and/or cellular apoptosis (2). Aberrant cellular proliferation, as manifested in cancer, can often be attributed to loss of correct cell cycle control (reviewed in refs. 3, 4). CDK2/cyclin E, CDK4/cyclin D, and CDK6/cyclin D primarily regulate progression from G_1 to S phase of the cell cycle. CDK2/cyclin A and CDK1/cyclin A primarily function during S phase and control progression through G_2. The CDK1/cyclin B complex is a key initiator of mitosis (5, 6). CDKs phosphorylate and modulate the activity of a wide variety of proteins required for cell cycle progression (7–10). CDK2/cyclin E also plays a role in the p53-mediated DNA damage response pathway and in gene regulation via c-Myc. Thus, affecting CDK1 and CDK2 activity may affect cell growth and survival via several mechanisms (11, 12).

A second group of CDKs, which include CDK7 and CDK9, are involved in transcriptional regulation independently of the cell cycle. Acting via phosphorylation of the COOH-terminal domain of RNA polymerase II, they promote initiation and elongation of nascent mRNA transcripts (13). Inhibition of the transcriptional CDKs has attracted interest because the most sensitive transcripts are those with short half-lives that encode cell cycle regulators, mitotic regulatory kinases, nuclear factor-κB-responsive gene transcripts, and apoptosis regulators, such as MCL-1 and X-linked inhibitor of apoptosis (14, 15). Diminution of levels of these transcripts and their encoded proteins may produce anticancer activity or augment apoptotic responses. CDKs as a family therefore represent attractive targets for therapeutics designed to arrest, or recover control of, the cell cycle in aberrantly dividing cells. Accumulating evidence from small interfering RNA studies and from genetic knockouts of the CDKs or their cyclin partners suggests a considerable degree of redundancy in their regulation of key cell cycle events (16–20). Indeed, viable mice exhibiting only a small number of nonlethal defects were obtained from individual knockout studies with CDK2, CDK4, and CDK6. These data were confirmed by antisense depletion of CDK2 or expression of a dominant-negative form of the kinase in human cancer cells (17). In these scenarios, CDK2 is dispensable for cell proliferation. The mouse knockout of CDK1, however, is nonviable and it is postulated that the ability of other CDKs, particularly CDK1, to interact with several cyclin partners is a key driver of redundancy. This theory is backed up by the observation that the knockout of

individual E/A-type cyclins results in an embryonic lethal phenotype (21). Further data showed that depletion of CDK1 or CDK2 alone by RNA interference in human cancer cells was insufficient to cause complete cell cycle blockade (22). Combined depletion of the CDKs had a markedly increased effect resulting in either G_2-M blockade or induction of apoptosis depending on the cell line in question. Pharmacologic inhibition of a kinase *in situ* is somewhat different to the loss of the protein entirely, which may enable the promiscuous binding of its partner cyclin to a CDK other than its usual partner.

Several drug discovery programs have produced potent small-molecule inhibitors of CDKs. In general, these have been focused on identifying inhibitors of CDK4 and/or CDK6 or on optimizing for inhibition of CDK2. Several of these compounds have entered clinical development and among the most advanced are flavopiridol, seliciclib (CYC-202/*R*-roscovitine), and SNS-032 (23–25). Each has been progressed against several indications in both solid and hematologic malignancies. Flavopiridol has shown clinical activity in chronic lymphocytic leukemia (26, 27). SNS-032 is reported to be in phase I/II development in advanced breast cancer, melanoma, non-small cell lung cancer, and B-cell malignancies (28, 29). Seliciclib is in phase II clinical studies in several indications (reviewed in ref. 29).

CDK2 was chosen by Astex as the basis for an integrated crystallography-based approach for the detection of high efficiency binding of low molecular weight fragments and their subsequent optimization using structure-based drug design into potent novel lead compounds (30). Soaking cocktails of fragments with apo-crystals of CDK2 identified several start points for chemistry. Optimization of one of these start points identified AT7519 as a potent inhibitor of CDKs, which was found to have antitumor activity in animal models of cancer (31). Here, we describe the further biological characterization of AT7519 in models of human cancer *in vitro* and *in vivo*.

Materials and Methods

AT7519

AT7519 is *N*-(4-piperidinyl)-4-(2,6-dichlorobenzoyla-mino)-1H-pyrazole-3-carboxamide synthesized by Astex Therapeutics (31).

In vitro Kinase Assays

Kinase assays were done according to methods outlined in Supplementary Data.[1]

Cell Culture and Reagents

Cell lines were obtained from European Collection of Cell Cultures (ECACC), American Type Culture Collection, or Deutsche Sammlung von Mikroorganismen und Zellkulturen. HCT116, HT29, A549, and MCF-7 (ECACC), MDA-MB-468 and SK-BR3 (American Type Culture Collection), and Granta-519 (Deutsche Sammlung von Mikroorganismen und Zellkulturen) were grown in DMEM. A2780,

HL60, K562, and MOLT-4 (ECACC), NCI-H69, NCI-H82, Ramos, and HCC1937 (American Type Culture Collection), and JEKO-1, F36-P, Kasumi-1, MOLM-13, and PL21 (Deutsche Sammlung von Mikroorganismen und Zellkulturen) were grown in RPMI 1640. SK-OV-3 (American Type Culture Collection) and MESSA (ECACC) cells were grown in McCoy's 5A medium and BT-20 (American Type Culture Collection) and MRC-5 (ECACC) cells grown in MEM. SW620 (ECACC) were grown in L15 medium and MV4-11 (Deutsche Sammlung von Mikroorganismen und Zellkulturen) was grown in Iscove's modified Dulbecco's medium. In all cases, medium was supplemented with 10% to 20% fetal bovine serum and cells were maintained at 37°C in an atmosphere of 5% CO_2. All reagents were purchased from Invitrogen UK unless otherwise stated.

Proliferation Assays

In all proliferation assays, cells were seeded into 96-well plates at 5×10^3 per well before addition of compound in 0.1% DMSO for 72 h. For the nonproliferating MRC-5 cell assays, cells were seeded at 1×10^4 per well and grown to confluence for 72 h before addition of compound in 0.1% DMSO for a further 72 h. In both cases, 10% (v/v) Alamar Blue (Biosource International) was added following compound incubation and cells incubated for a further 6 h. Plate fluorescence was read at $\lambda_{ex} = 535$ nm and $\lambda_{em} = 590$ nm.

Western Blotting

HCT116 cells were seeded at a concentration of 0.5×10^6/mL medium onto 6-well tissue culture plates and allowed to recover for 16 h. AT7519, at the indicated concentration, or vehicle control (0.1% DMSO) was added for 24 h. Cells were harvested and lysed in 100 μL ice-cold Triton X-100 lysis buffer [0.1% (v/v) Triton X-100]. Lysates were cleared by centrifugation and a sample of the supernatant was removed for protein determination. Equivalent amounts of protein lysate had SDS sample buffer added and were boiled for 5 min. Samples were resolved by SDS PAGE (NuPage System, Invitrogen) and blotted onto polyvinylidene difluoride filters. Immunoblotting was done with the specific antibodies described. Anti-phospho-protein phosphatase 1α (PP1α), protein phosphatase 1α, CDK1, phospho-nucleophosmin (NPM), and phospho-retinoblastoma (Rb; T^{780}) antibodies were from Cell Signalling Technology. Anti-total Rb and anti-phospho-Rb (T^{821}) were from Biosource International. RNA polymerase II antibodies were from Cambridge Bioscience. Detection was achieved using ECL^{PLUS} reagents (Amersham Bioscience).

Apoptosis Assays

For colony formation assays, 50 cells/mL medium were seeded onto 6-well tissue culture plates and allowed to recover for 16 h. AT7519 or vehicle control (0.1% DMSO) was added for the indicated time. Following compound treatment, medium was replaced without compound and colonies were allowed to grow out for 14 days. During this time, medium was replenished every 4 to 5 days. Colonies were fixed in 2 mL Carnoy's fixative (25% acetic acid, 75% methanol) and stained in 2 mL of 0.4% (w/v) crystal violet. The number of colonies in each well was counted and expressed as a percentage of the control.

---

[1] Supplementary material for this article is available at Molecular Cancer Therapeutics Online (http://mct.aacrjournals.org/).

Cell Cycle Analysis

For cell cycle analysis in an asynchronous population, 0.5×10^6 cells/mL medium were seeded onto 6-well tissue culture plates and allowed to recover for 16 h. AT7519 or vehicle control (0.1% DMSO) was added for 24 h. Cells were harvested and fixed in 2 mL of 70% ethanol. Cells were collected by centrifugation and washed with 1 mL PBS. Samples were centrifuged again and resuspended in 1 mL PBS containing 50 μg/mL propidium iodide and 0.1 mg/mL RNase. Cells were incubated at 37°C for 30 min and then analyzed by flow cytometry to determine propidium iodide incorporation using a BD FACSCalibur and CellQuest Pro analysis software. In the case of block and release experiments, cells were seeded at a concentration of 0.5×10^6 per plate onto 10 cm dishes (MRC-5) or 3×10^5 per well onto a 6-well plate (HCT116) and allowed to recover overnight. Cells were transferred to serum-free medium for 24 h or treated with 2 mmol/L thymidine for 16 h as indicated. Following cell cycle arrest, cells were returned to complete, fresh medium containing AT7519 for various times as indicated in the figures below. Following incubation, cells were harvested and analyzed as above.

Pharmacodynamic Studies

S.c. xenograft tumors were removed from nude mice at the indicated times following administration of a single i.p. dose of 10 mg/kg AT7519. Tumor samples were ground to a fine powder under liquid nitrogen and protein was extracted by addition of 1 mL Triton X-100 lysis buffer. Western blots were done as outlined in Materials and Methods above.

Pharmacokinetic Studies

AT7519 was dissolved in saline and administered via the i.v. route to male BALB/c nude mice bearing HCT116 tumor xenografts at a dose level of 5 mg/kg as free base equivalents. Triplicate plasma and tumor samples were obtained at timed intervals up to 16 h following compound administration and prepared for bioanalysis by protein precipitation. Quantitation was by liquid chromatography-tandem mass spectrometry using an AT7519-specific method monitoring the transition m/z 382.02→84.08 in positive ion mode. Pharmacokinetic variables were determined using WinNonLin v4.1 (Pharsight).

Xenograft Models

Experiments on mice bearing HCT116 xenografts were done by Molecular Imaging Research. Female ICR severe combined immunodeficient mice were purchased from Taconic Farms and housed in pathogen-free conditions according to procedures approved by MIR Animal Care and Use Committee. Four-week-old animals were implanted s.c. on day 0 with 30 to 60 mg tumor fragments using a 12-gauge Trocar. Treatment started on day 12 after implantation for the early-stage HCT116 xenograft study (tumor volume range, 75-150 mm³; 8 mice per group) and on day 15 for the study using advanced-stage tumors (275-550 mm³; 12 mice per group). Mice were dosed according to schedule. Tumor dimensions were measured every 2 or 3 days and the volume was calculated according to the equation: length × width² × 0.5. Experiments using male BALB/c *nu/nu* mice

were done according to UK Animals (Scientific Procedures) Act 1986. Animals were purchased from Harlan UK and housed in pathogen-free conditions. Six- to 8-week-old male BALB/c Hsd:athymic nude-*Foxn1*[nu] mice were implanted s.c. with one HT29 tumor fragment per mouse into the right flank. Five days after implantation, mice were arranged into groups of 12 according to tumor volume with a mean volume of 75 mm³ (range, 50-130 mm³). Mice were then dosed according to schedule. Tumor volume was measured every 2 to 3 days as above.

In each case, a statistically significant slowing of increase in xenograft volume or regression of tumor volume over time compared with a matched control group was used to characterize efficacy. A complete regression was defined as a decrease in tumor volume to an undetectable size, taken as measurements of <3 mm in any dimension. Tolerability was estimated by monitoring body weight loss, clinical signs, and survival over the course of the study.

Results

Identification of AT7519 as a CDK Inhibitor

An integrated crystallography-based approach was employed for the identification of low molecular weight fragments that bound CDK2 with high efficiency. These hits were subsequently optimized using structure-based drug design into potent novel lead compounds. One of these compounds, AT7519, is a potent inhibitor of several CDKs and was selected for clinical development (Fig. 1A; ref. 31). The inhibitory activity of AT7519 was assayed against several isolated kinases *in vitro* (Supplementary Table S1).[1] AT7519 potently inhibited CDK1, CDK2, CDK4 to CDK6, and CDK9 with IC50 values of 210, 47, 100, 13, 170, and <10 nmol/L, respectively. The compound had lower potency against other CDKs tested (CDK3 and CDK7) and was inactive against all of the non-CDK kinases tested with the exception of GSK3β (89 nmol/L). The inhibition of CDK1 by AT7519 is competitive with ATP, with a K_i value of 38 nmol/L (data not shown). This observation is consistent with the X-ray structure of a complex of CDK2 and AT7519, confirming that AT7519 binds within the active site cleft of the enzyme overlapping with the ATP-binding site (31).

In vitro Cellular Activity of AT7519

The antiproliferative activity of AT7519, following 72 h compound exposure, was determined against a variety of human tumor cell lines (Table 1). AT7519 potently inhibited proliferation irrespective of tumor cell source with IC50 values ranging from 40 to 940 nmol/L for the 26 tumor cell line types tested. Of particular note is that the compound was effective against cell lines expressing a mutant form of the tumor suppressor p53 (HT29 and MDA-MB-468). The p53 independence of the antiproliferative effect of AT7519 was confirmed in the HCT116 N7 cell line in which the p53 pathway is suppressed. The antiproliferative IC50 of AT7519 against this cell line was equivalent to that observed for wild-type HCT116 cells (data not shown). In addition, MDA-MB-468 cells that lack the Rb protein
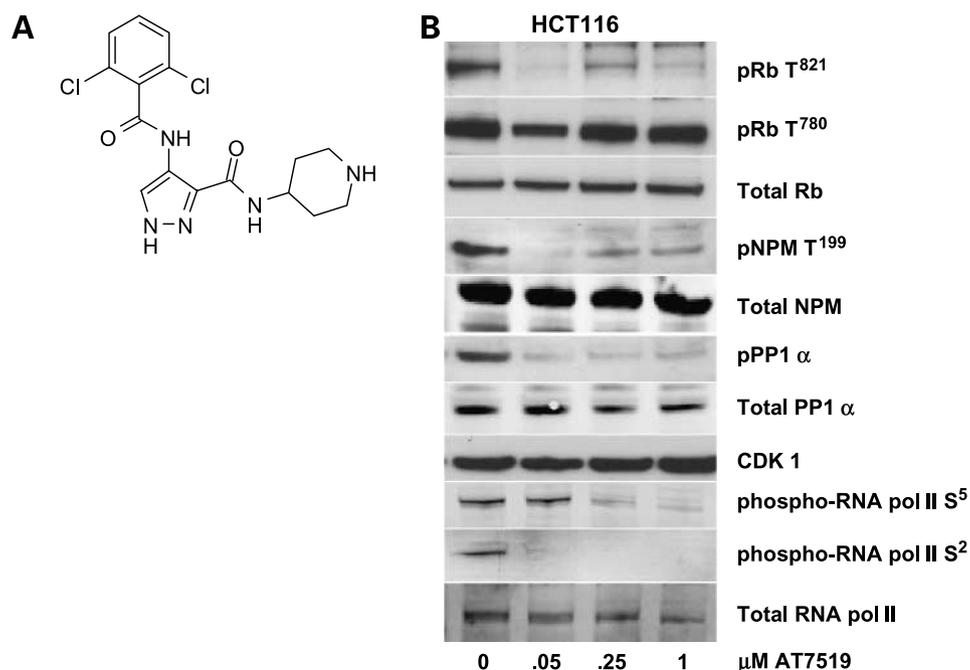
Figure 1. Chemical structure of AT7519 (**A**). HCT116 cells were treated for 24 h with AT7519 and lysates were prepared for Western blotting. Representative of three independent experiments (**B**).

remained sensitive to AT7519. Because functional Rb is required for CDK4 inhibition to result in cell cycle arrest (reviewed in ref. 32), this suggests that the anti-CDK4 activity of AT7519 alone is not responsible for the antiproliferative effects. In contrast to the compound's potent activity against cycling tumor cell lines, AT7519 did not affect the viability of noncycling MRC-5 cells at concentrations up to 10 μmol/L. These data suggest that the mechanism by which the compound exerts its effect is cell cycle related and the compound is not generally cytotoxic to cells that are not dividing.

The mechanism of action of AT7519 in cells has been investigated by monitoring the phosphorylation state of substrates specific for the various CDKs within treated HCT116 cells (Fig. 1B). These studies indicated that inhibition of cellular CDK1 and CDK2 by AT7519 was observed at concentrations consistent with the observed antiproliferative effects. Treatment with AT7519 for 24 h was sufficient to inhibit phosphorylation of the CDK1 substrate PP1α (T^{320}) and the CDK2 substrates Rb (T^{821}) and NPM (T^{199}) in HCT116 cells. Additional studies showed phosphorylation of NPM and Rb to be inhibited following a 1 h exposure to AT7519 (data not shown), suggesting that these inhibitory effects on substrate phosphorylation were a direct effect of CDK inhibition rather than a consequence of cell cycle arrest. No effect of AT7519 was observed on the cyclin D-dependent phosphorylation site on Rb (S^{780}) in cell-based systems despite the observation in cell-free kinase assays that the com-

pound inhibited CDK4/cyclin D activity (Supplementary Table S1).[1] This supports the previous observation in Rb-negative cells (MDA-MB 468) that inhibition of CDK4 by AT7519 was not responsible for its antiproliferative effects. Levels of the relevant cyclins, CDKs, and total proteins remained unaffected by compound treatment. The effects of the compound on phosphorylation of the COOH-terminal domain repeats of RNA polymerase II were also assessed. AT7519 inhibited phosphorylation of RNA polymerase II on Ser^2 of the COOH-terminal domain, indicating that AT7519 has the potential to inhibit transcription downstream of the polymerase, consistent with the observed *in vitro* inhibition of CDK9. Inhibition of total transcription was assayed using tritiated uridine incorporation into RNA and showed that a 4 h treatment of HCT116 cells with AT7519 was sufficient to inhibit global transcription with an IC_{50} of 56 nmol/L (data not shown), similar to the levels required for inhibition of proliferation (Table 1).

AT7519 Inhibits Cell Cycle Progression in Human Tumor Cell Lines

The effect of AT7519 on cell cycle progression was investigated in HCT116 cells. Cells treated for 24 h with increasing concentrations of AT7519 showed a significant reduction in the number of cells in S phase and an increase in the number of cells in G_2-M (Fig. 2A). Colabeling with bromodeoxyuridine and propidium iodide showed that cells were also arrested in the G_0-G_1 phase of the cell cycle (data not shown). An increase in cells containing sub-G_1

amounts of DNA was observed, indicating that the compound was inducing cell death. AT7519-induced G_0-G_1 and G_2-M cell cycle blockade was confirmed by releasing the cells from serum deprivation or thymidine-induced cell cycle arrest in the presence of compound. Cells arrested in G_0-G_1 by serum deprivation were unable to reenter the cell cycle on readdition of serum in the presence of 250 nmol/L AT7519 (Fig. 2B). Cells arrested in late G_1 or early S phase by thymidine treatment reentered the cell cycle in the presence of AT7519. There appears to be a delay in the progress of S phase, but subsequently all cells accumulated in G_2-M (Fig. 2C). A similar pattern of cell cycle arrest was shown in several other cell lines including the Rb-negative MDA-MB-468 cell line (data not shown).

Induction of Apoptosis by AT7519 in Human Tumor Cell Lines

The induction of apoptosis by AT7519 was confirmed with colony formation and TUNEL staining assays. HCT116, HT29, and A2780 cells were exposed to AT7519

Table 1. Antiproliferative activity of AT7519 in a panel of human tumor cell lines

Tissue	Cell line	Inhibition of proliferation IC$_{50}$ (nmol/L)
Colon carcinoma	HCT116	82
	HT29	170
	SW620	940
Ovarian carcinoma	A2780	350
	SK-OV-3	400
Lung carcinoma	A549	310
	NCI-H69	330
	NCI-H596	690
	NCI-H82	230
Breast carcinoma	MCF-7	40
	BT-20	320
	MDA-MB-468	340
	SK-BR3	140
	HCC1937	460
Uterine sarcoma	MESSA	660
Leukemia	HL60	230
	K562	310
	MOLT-4	310
	F36-P	390
	Kasumi-1	250
	MOLM-13	170
	MV4-11	170
	PL-21	160
Lymphoma	Granta-519	160
	JEKO-1	670
	Ramos	720
Fibroblast	MRC-5	980
	MRC-5 (nonproliferating)	>10,000

NOTE: Exponentially growing cells were exposed to compound for 72 h before determination of viable cell number by the addition of Alamar Blue reagent. In the case of the nonproliferating MRC-5 cells, they were grown to confluence before addition of the compound to measure compound effects in the absence of proliferation. Experiments were done in triplicate and data are mean of at least two independent experiments.

at concentrations corresponding to the antiproliferative IC$_{50}$ or IC$_{90}$ for that cell line (Table 2). In each case, an exposure time of 24 h, which is equivalent to or greater than one cell cycle, was required to observe substantial induction of apoptosis. This was consistent with the compound inducing apoptosis in a cell cycle-dependent manner, perhaps requiring AT7519 to be present during a certain point(s) in the cell cycle to drive the apoptotic response. This pattern of induction of apoptosis was confirmed by the TUNEL assay in the HCT116 cells (data not shown).

Pharmacokinetic Studies

Average plasma and tumor pharmacokinetic variables determined in tumor-bearing nude mice are given in Supplementary Table S2[1] and a graphical representation of the concentration-time profiles is shown in Fig. 3. The half-life in tumor tissue was approximately three times longer than in plasma (3 versus 1.1 h). The half-life of AT7519 in tumor after i.p. dosing was identical to that obtained after i.v. administration (data not shown). Plasma clearance was moderate at 55 mL/min/kg, being ~60% of liver blood flow in the mouse. Bioavailability following i.p. administration was essentially complete (data not shown). Protein binding in mouse plasma *in vitro* was 42 ± 6% at 1 μg/mL, and 61% to 70% of AT7519 was associated with the cellular component of mouse blood giving a blood-to-plasma ratio of 2.0 ± 0.1 at 0.5 μg/mL and 1.8 ± 0.2 at 5 μg/mL.

Activity in Human Tumor Xenograft Models

AT7519 inhibited the growth of early-stage HCT116 tumor xenografts at doses of 4.6 and 9.1 mg/kg/dose when given twice in a 24 h period, at 0 h, 8 h later, and 24 h following initial dose for 9 consecutive days (Fig. 4A). Under the 9.1 mg/kg dosing regimen, all animals achieved complete tumor regression for between 5 and 24 days with T/C values of 1% on day 14 (i.p. route) or 2% on day 15 (i.v. route) and tumor growth delay of 31 to 34 days. One mouse in the 9.1 mg/kg group remained tumor-free at the end of the study period. Growth curves became significantly different from control ($P < 0.05$) on day 4 for 9.1 mg/kg dosing by the i.v. route and on day 6 for the i.p. route. The efficacy achieved by the i.v. or i.p. route was essentially indistinguishable. The 4.6 mg/kg/dose group (i.v. route) gave a T/C value of 45% and a tumor growth delay of 7 days with growth curves becoming significantly different from controls ($P < 0.05$) on day 11. Treatment with a dose of 2.3 mg/kg (i.v. route) was without effect. All doses were well tolerated.

The efficacy of AT7519 against advanced-stage HCT116 tumor xenografts in severe combined immunodeficient mice dosed with 9.1 mg/kg twice daily for 9 consecutive days was examined (Fig. 4B). Tumor regression was observed with complete regression in 6 of 8 mice within the group with 1 mouse remaining tumor-free for the complete study period. Growth curves of the treated animal groups became significantly different from control ($P < 0.05$) on day 2 and a T/C value of 16% was obtained.

In early-stage HCT116 xenografts, dosing for 3 days was the minimum period required to achieve efficacy, consistent with persistence of benefit off-treatment (data
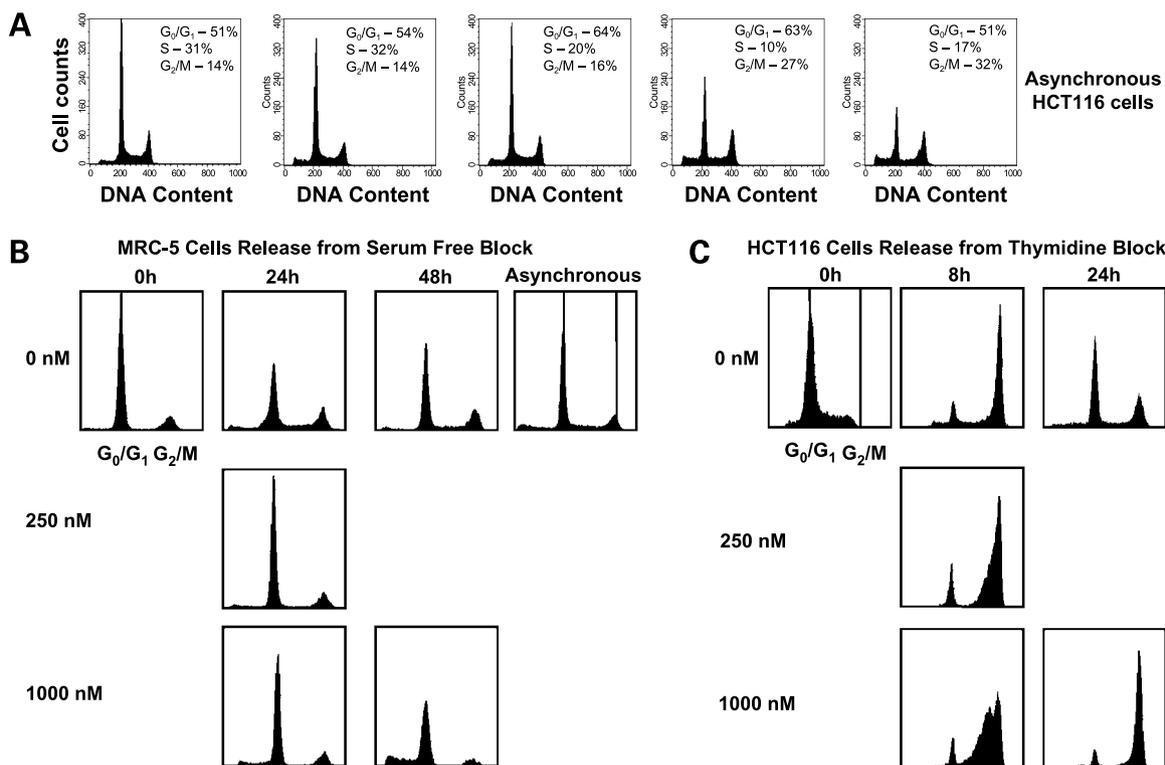
Figure 2. AT7519 treatment causes a G_0-G_1 and G_2-M cell cycle arrest. Treatment of an asynchronous population of HCT116 cells resulted in an accumulation of cells in the G_2-M phase of the cell cycle following 24 h compound treatment (**A**). Human fibroblast cells (MRC-5) arrested in G_0 by withdrawal of serum from the medium for 48 h were transferred to medium containing 10% fetal bovine serum and AT7519 or vehicle control (**B**) for the times and at the concentrations indicated on the *x* and *y axes*, respectively. HCT116 cells arrested in G_1 with treatment of 2 mmol/L thymidine were transferred to medium containing 10% fetal bovine serum and AT7519 or vehicle control (**C**) for the times and at the concentrations indicated on the *x* and *y axes*, respectively. The effect of AT7519 on the release of cells from these cell cycle blockades was assessed by flow cytometry. Representative of two independent experiments.

not shown). Longer periods of dosing produced more dramatic efficacy and a longer period of benefit off-treatment. Treatment with AT7519 at doses of 5 and 7.5 mg/kg/dose given twice daily for 9 consecutive days inhibited the growth of early-stage HT29 tumor xenografts

Table 2. AT7519 induces apoptosis in human tumor cell lines

Cell line	Treatment time (h)	% Control survival, IC_{50}	% Control survival, IC_{90}
HCT116	8	89 ± 9	45 ± 8
	24	52 ± 7	0 ± 0
A2780	8	50 ± 2	18 ± 4
	24	3 ± 1	0 ± 0
HT29	8	94 ± 12	66 ± 14
	24	94 ± 23	23 ± 7

NOTE: The induction of apoptosis in several human tumor cell lines was assessed using a colony formation assay. Cell lines were plated out and exposed to compound at concentrations relating to the IC_{50} and IC_{90} for the indicated times. The number of colonies growing through following compound exposure were determined and compared to vehicle control. Data are the percentage of colonies observed in compound-treated wells compared with the numbers observed in vehicle control wells. Mean $\pm$ SD of three independent experiments.

(Fig. 4C) with T/C values being 32% and 12% for the 5 and 7.5 mg/kg groups, respectively. Growth curves became significantly different from control ($P < 0.01$) from day 8 onwards and 2 of 12 mice showed complete regression in the 7.5 mg/kg dose group on day 12.

Pharmacodynamic Effects of AT7519 in Tumor Xenograft Models

Inhibition of the target CDKs by AT7519 in tumor xenografts was confirmed by investigating the phosphorylation of the CDK2 substrates NPM and Rb in tumors from treated animals. HCT116 tumor-bearing BALB/c nude mice were treated with a single dose of AT7519 at 10 mg/kg i.p. Tumors were removed at various times following dosing and the levels of the pharmacodynamic marker were determined. Figure 4D shows the results of analysis for phospho-NPM and the apoptosis marker, cleaved PARP, by Western blotting. Total NPM was monitored as a loading control. Phosphorylation of NPM (T^{199}) was inhibited at 0.5 and 1 h after AT7519 treatment and the apoptosis marker, cleaved poly (ADP-ribose) polymerase (PARP), was increased at 16 and 24 h post-treatment. Phosphorylation of the CDK substrates Rb and NPM and levels of the proliferation marker Ki-67 were also monitored by fluorescent immunohistochemistry in tumor

Figure 3. Plasma and tumor AT7519 concentration-time profiles in BALB/c nude mice bearing HCT116 xenografts after i.v. administration at 5 mg/kg. Mean ± SE of $n = 3$ per time point, except at 0.25 h where $n = 1$.

samples from mice bearing HCT116 xenografts after administration of AT7519. Tumor-bearing mice were dosed with 10 mg/kg i.p. AT7519 and tumors were removed at various times post-treatment. Inhibition of all markers was observed at 1 to 3 h following treatment, correlating with the data obtained by Western blotting (data not shown).

Measurement of AT7519 concentration-time and pharmacodynamic marker-time courses allowed characterization of the exposure and effect relationship in tumor xenograft models. Suppression of phospho-NPM for a limited time is sufficient to induce an apoptopic response in at least a subset of cells depending on their position in the cell cycle. Repeated intermittent administration of AT7519 is proposed to affect increasingly large proportions of tumor cells leading to the regression observed in tumor xenograft models. Intermittent cyclic dosing schedules were found to provide the best efficacy and tolerability (therapeutic index) and were therefore proposed for investigation in early clinical studies.

Discussion

AT7519 potently inhibits CDK1, CDK2, CDK4 to CDK6, and CDK9 with lower potency against other CDKs evaluated (CDK3 and CDK7) and was inactive against most non-CDK kinases. Exposure of tumor cells to AT7519 results in cell cycle arrest and, ultimately, cell death by apoptosis. The compound has potent antiproliferative activity in a variety of human tumor (but not nonproliferating) cell lines *in vitro*,
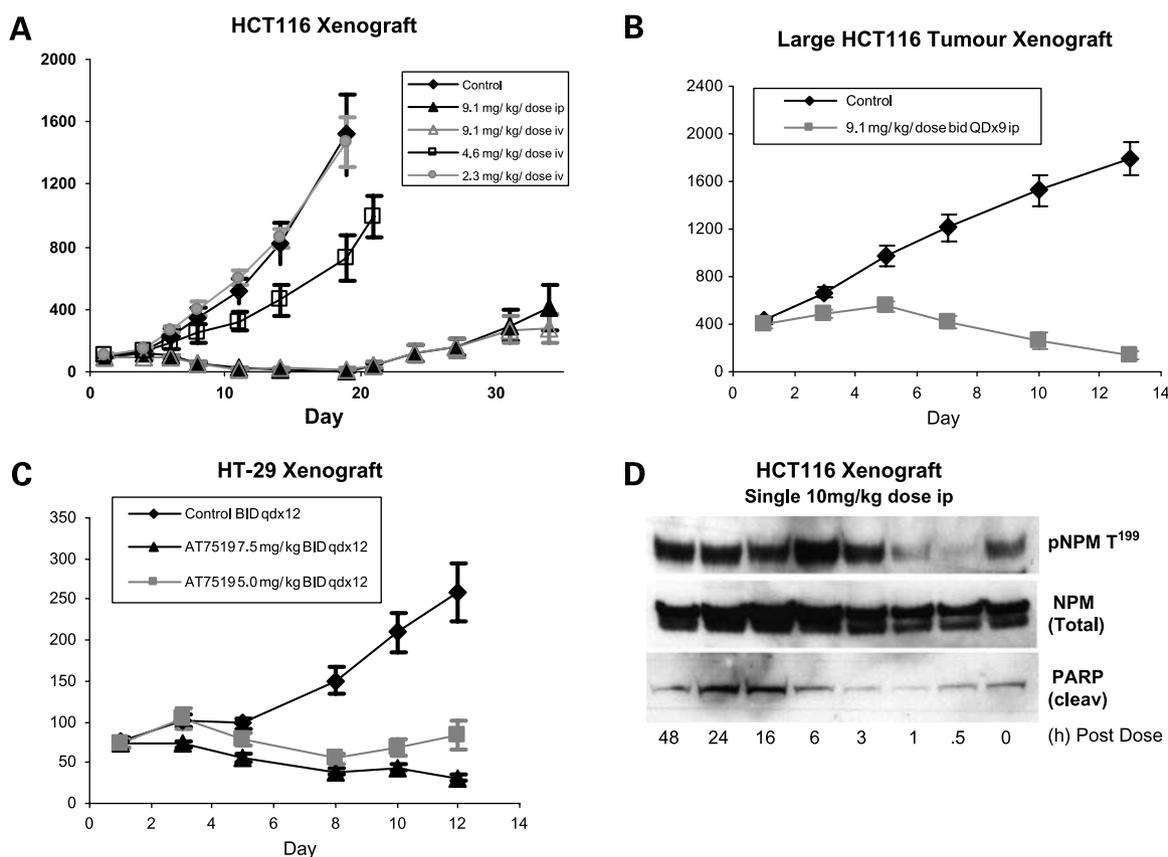

Figure 4. Severe combined immunodeficient mice bearing HCT116 tumors (**A**) or nude mice bearing HT29 tumors (**C**) were given twice daily administration of AT7519 by the route described and at the indicated doses for 9 d. **B,** HCT116 tumors were allowed to grow to ~400 mm before initiation of dosing as indicated. **D,** HCT116 tumor xenografts were given a single dose of AT7519 at 10 mg/kg. Mean ± SE growth curves for groups of $n = 8$ (**A**), $n = 12$ (**B**), or $n = 12$ (**C**). Tumors were removed at the indicated times following dosing and Western blotting was done for markers of CDK inhibition.

which occurs in parallel with inhibition of CDK1 and CDK2 as judged from inhibition of phosphorylation of specific substrates for these kinases in cell-based systems. The fact that AT7519 has an antiproliferative action in Rb-negative cell lines and induces the same pattern of cell cycle arrest in both wild-type and Rb-negative cell lines such as MDA-MB 468 suggests that the CDK4 inhibitory activity of the compound is not a contributing factor to its antiproliferative effects. Selective CDK4 inhibitors would be expected to be ineffective at inhibiting the proliferation of cell lines lacking Rb, the only known substrate of CDK4.

In common with other inhibitors of this class, AT7519 inhibits transcription downstream of RNA polymerase II. The mechanism of this effect was proposed to be via inhibition of phosphorylation of serine in the COOH-terminal domain repeat domains of the polymerase (13–15). We cannot discount the possibility that this activity of AT7519 contributes to its efficacy in the *in vitro* and *in vivo* models tested. It is possible that transcriptional regulation is an additional mechanism by which the compound may exert its cell cycle effect through modulation of transcriptionally regulated cell cycle proteins or by direct induction of apoptosis; however, several studies *in vitro* showed a requirement for compound coverage over a complete cell cycle for AT7519 to exert its maximal proapoptotic effect. Also, CDK inhibitors exerting effects via a transcriptional mechanism induce rapid apoptosis in the absence of cell cycle arrest (23, 24). These data suggest that the mechanism of action of AT7519, in the cell lines studied here, is consistent with it acting in a cell cycle-dependent manner via inhibition of CDK1 and CDK2.

The aggressive antitumor properties of AT7519 are most clearly seen in xenograft tumor models, where it caused regression of both early-stage (100 mm^3) and advanced-stage (400 mm^3) s.c. tumors. Pharmacodynamic markers showed that this tumor kill effect was associated with increased levels of tumor apoptosis and at doses in mice that induced only a transient inhibition of substrate phosphorylation markers in the tumors. In comparison with published data for other CDK inhibitors in this class, AT7519 appears to be more effective in the extent to which it can induce tumor regression following a short period of treatment. CYC-202 was reported to cause a 45% or 62% tumor growth reduction when administered by the i.p. route to mice bearing Lovo colorectal xenografts or by the oral route to mice bearing MESSA DX-5 uterine sarcoma xenografts, respectively. No regressions were reported using these optimal schedules (33). Similarly, flavopiridol administered on an optimized scheduled caused sustained tumor growth inhibition of ~60% without evidence of regression in the HN12 xenograft model (34). Newer-generation compounds, such as R547 (35) and P276-00 (36) from Hoffmann-La Roche and Nicholas Piramal, exhibited maximal *in vivo* growth inhibitions of 60% and 80%, respectively, in several models; but again, no regressions were reported. Similarly, CDKi-277 from Amgen was reported to give cytostasis with regressions observed only at nontolerated doses (37). The antitumor effects of AT7519

continued after treatment ended, with the duration of the off-treatment effect being dependent on the initial size of the tumor and duration and frequency of the dose level administered. Although no tumors were detectable for up to 10 days off-treatment in some studies, most tumors eventually grew again. Complete tumor regressions were achieved in two individual mice from the HCT116 studies; in one case, the mouse remained tumor-free >20 days following the final dose of AT7519. Studies were not done to investigate whether the nature of the tumor changed on regrowth and whether they maintained sensitivity to AT7519. Optimization of the first cycle of treatment to achieve the best therapeutic index showed that at least twice daily doses over a minimum period of 3 days were required for prolonged off-treatment benefit.

The CDKs and several key regulatory components are often deregulated in human tumors, and as such, they offer an attractive therapeutic target for novel small-molecule therapies. The encouraging biological profile and excellent *in vivo* efficacy of this compound supports the biological rationale behind the clinical studies initiated with this compound.

Disclosure of Potential Conflicts of Interest

The authors hold shares and share options in Astex Therapeutics Ltd. No other potential conflicts of interest were disclosed.

References

1. Sherr CJ. Cancer cell cycles. Science 1996;274:1672–7.

2. Grana X, Reddy EP. Cell cycle control in mammalian cells: role of cyclins, cyclin-dependent kinases (CDKs), growth suppressor genes and cyclin-dependent kinase inhibitors (CKIs). Oncogene 1995;11:211–9.

3. Malumbres M, Barbacid M. To cycle or not to cycle: a critical decision in cancer. Nat Rev Cancer 2001;1:222–31.

4. Morgan D. Principles of CDK regulation. Nature 1995;374:131–4.

5. Dohadwala M, Da Cruz E, Silva E, et al. Phosphorylation and inactivation of protein phosphatase 1 by cyclin-dependent kinases. Proc Natl Acad Sci U S A 1994;91:6408–12.

6. Kwon Y, Lee S, Choi Y, Greengard P, Nairn AC. Cell cycle-dependent phosphorylation of mammalian protein phosphatase 1 by cdc2 kinase. Proc Natl Acad Sci U S A 1997;94:2168–73.

7. Brown VD, Phillips RA, Gallie BL. Cumulative effect of phosphorylation of pRb on regulation of E2F activity. Mol Cell Biol 1999;19:3246–56.

8. Harbour JW, Luo RX, Dei Santi A, Postigo AA, Dean DC. CDK phosphorylation triggers sequential intramolecular interactions that progressively block Rb functions as cells move through G$_1$. Cell 1999;98:859–69.

9. Zhao J, Dynlacht B, Imai T, Hori T, Harlow E. Expression of NPAT, a novel substrate of cyclin E-CDK2, promotes S-phase entry. Genes Dev 1998;12:456–61.

10. Zhao J, Kennedy B, Lawrence BD, et al. NPAT links cyclin E-CDK2 to the regulation of replication-dependent histone gene transcription. Genes Dev 2000;14:2283–97.

11. Santoni-Rugiu E, Falck J, Mailand N, Bartek J, Lukas J. Involvement of Myc activity in a G$_1$/S-promoting mechanism parallel to the pRb/E2F pathway. Mol Cell Biol 2000;20:3497–509.

12. Obaya Aj, Kotenko I, Cole MD, Sedivy JM. The proto-oncogene cmyc acts through the cyclin-dependent kinase (CDK) inhibitor p27^{KIP1} to facilitate the activation of CDK4/6 and early G$_1$ phase progression. J Biol Chem 2002;277:31263–9.

13. Pinhero R, Liaw P, Bertens K, Yankulov K. Three cyclin dependent kinases preferentially phosphorylate different parts of the C-terminal domain of the large subunit of RNA polymerase II. Eur J Biochem 2004;271:1004–14.

14. Garriga J, Grana X. Cellular control of gene expression by T-type cyclin/CDK9 complexes. Gene 2004;337:15 – 23.

15. Lam LT, Pickeral OK, Peng AC, et al. Genomic-scale measurement of mRNA turnover and the mechanisms of action of the anti-cancer drug flavopiridol. Genome Biol 2001;2:1 – 11.

16. Berthet C, Aleem E, Coppola V, Tessarollo L, Kaldis P. CDK2 knockout mice are viable. Curr Biol 2003;13:1775 – 85.

17. Tetsu O, McCormick F. Proliferation of cancer cells despite CDK2 inhibition. Cancer Cell 2003;3:233 – 45.

18. Ortega S, Prieto I, Odajima J, et al. Cyclin-dependent kinase 2 is essential for meiosis but not for mitotic cell division in mice. Nat Genet 2003;35:25 – 31.

19. Geng Y, Yu Q, Sicinska E, et al. Cyclin E ablation in the mouse. Cell 2003;114:431 – 43.

20. Malumbres M, Sotillo R, Santamaria D, et al. Mammalian cells cycle without the D-type cyclin-dependent kinases CDK4 and CDK6. Cell 2004; 118:493 – 504.

21. Malumbres M, Barbacid M. Mammalian cyclin dependent kinases. Trends Biochem Sci 2005;30:630 – 41.

22. Cai D, Latham VM, Zhang X, Shapiro GI. Combined depletion of cell cycle and transcriptional cyclin-dependent kinase activities induces apoptosis in cancer cells. Cancer Res 2006;66:9270 – 80.

23. Carlson BA, Dubay MM, Sausville EA, Brizuela L, Worland PJ. Flavopiridol induces G_1 arrest with inhibition of cyclin-dependent kinase (CDK) 2 and CDK4 in human breast carcinoma cells. Cancer Res 1996;56: 2973 – 8.

24. Senderowicz AM. Novel small molecule cyclin-dependent kinases modulators in human clinical trials. Cancer Biol Ther 2003;2:S84 – 95.

25. Meijer L, Borgne A, Mulner O, et al. Biochemical and cellular effects of roscovitine, a potent and selective inhibitor of the cyclin-dependent kinases cdc2, cdk2 and cdk5. Eur J Biochem 1997;243: 527 – 36.

26. Christian BA, Grever MR, Byrd JC, Lin TS. Flavopiridol in the treatment of chronic lymphocytic leukemia. Curr Opin Oncol 2007;19:573 – 8.

27. Byrd JC, Lin TS, Dalton JT, et al. Flavopiridol administered using a pharmacologically derived schedule is associated with marked clinical efficacy in refractory, genetically high-risk chronic lymphocytic leukemia. Blood 2007;109:399 – 404.

28. Heath EI, Bible K, Martell RE, Adelman DC, Lorusso PM. A phase 1 study of SNS-032 (formerly BMS-387032), a potent inhibitor of cyclin-dependent kinases 2, 7 and 9 administered as a single oral dose and weekly infusion in patients with metastatic refractory solid tumors. Invest New Drugs 2008;26:59 – 65.

29. Malumbres M, Pevarello P, Barbacid M, Bischoff JR. CDK inhibitors in cancer therapy: what is next? Trends Pharmacol Sci 2008;29:16 – 21.

30. Blundell TL, Jhoti H, Abell C. High throughput crystallography for lead discovery in drug design. Nat Rev Drug Discov 2002;1:45 – 54.

31. Wyatt PG, Woodhead AJ, Berdini V, et al. Identification of *N*-(4-piperidinyl)-4-(2,6-dichlorobenzoylamino)-1H-pyrazole-3-carboxamide, (AT7519), a novel cyclin dependent kinase inhibitor using fragment based X-ray crystallography and structure based drug design. J Med Chem 2008; 51:4986 – 99.

32. Shapiro GI. Cyclin-dependent kinase pathways as targets for cancer treatment. J Clin Oncol 2006;24:1770 – 83.

33. McClue SJ, Blake D, Clarke R, et al. *In vitro* and *in vivo* antitumor properties of the cyclin dependent kinase inhibitor CYC202 (*R*-roscovitine). Int J Cancer 2002;102:463 – 8.

34. Patel V, Senderowicz AM, Pinto D, et al. Flavopiridol, a novel cyclin-dependent kinase inhibitor, suppresses the growth of head and neck squamous cell carcinomas by inducing apoptosis. J Clin Invest 1998;102: 1674 – 81.

35. DePinto W, Chu X, Yin X, et al. *In vitro* and *in vivo* activity of R457: a potent and selective cyclin-dependent kinase inhibitor currently in phase I clinical trials. Mol Cancer Ther 2006;5:2644 – 58.

36. Kalpana SJ, Rathos MJ, Mahajan P, et al. P276-00, a novel cyclin-dependent kinase inhibitor induces G_{1-2} arrest, shows anti-tumour activity on cisplatin-resistant cells and significant *in vivo* efficacy in tumour models. Mol Cancer Ther 2007;6:926 – 34.

37. Payton M, Chung G, Yakowec P, et al. Discovery and evaluation of dual CDK1 and CDK2 inhibitors. Cancer res 2006;66:4299 – 308.

AACR American Association
for Cancer Research

Molecular Cancer Therapeutics

Biological characterization of AT7519, a small-molecule inhibitor of cyclin-dependent kinases, in human tumor cell lines

Matthew S. Squires, Ruth E. Feltell, Nicola G. Wallis, et al.

Updated version	Access the most recent version of this article at: doi:10.1158/1535-7163.MCT-08-0890
Supplementary Material	Access the most recent supplemental material at: http://mct.aacrjournals.org/content/suppl/2009/01/23/1535-7163.MCT-08-0890.DC1 http://mct.aacrjournals.org/content/suppl/2018/08/10/1535-7163.MCT-08-0890.DC2

Cited articles	This article cites 36 articles, 15 of which you can access for free at: http://mct.aacrjournals.org/content/8/2/324.full#ref-list-1
Citing articles	This article has been cited by 10 HighWire-hosted articles. Access the articles at: http://mct.aacrjournals.org/content/8/2/324.full#related-urls

E-mail alerts	Sign up to receive free email-alerts related to this article or journal.
Reprints and Subscriptions	To order reprints of this article or to subscribe to the journal, contact the AACR Publications Department at pubs@aacr.org.
Permissions	To request permission to re-use all or part of this article, use this link http://mct.aacrjournals.org/content/8/2/324. Click on "Request Permissions" which will take you to the Copyright Clearance Center's (CCC) Rightslink site.